Electric polarizabilities of CH_4, CO, and O_2 determined by an optical refractometer

Metrologia

OPEN ACCESS

RECEIVED
6 January 2026

REVISED
20 February 2026

ACCEPTED FOR PUBLICATION
3 March 2026

PUBLISHED
17 March 2026

PAPER

Electric polarizabilities of CH_4, CO, and O_2 determined by an optical refractometer

Zi-Fan Zhao(赵子凡)[1], **Zhong-Liang Nie**(聂中梁)[2], **Jin Wang**(王进)[3,*] **and Shui-Ming Hu**(胡水明)[1,2,3]

[1] State Key Laboratory of Chemical Reaction Dynamics, Department of Chemical Physics, University of Science and Technology of China, Hefei 230026, People's Republic of China
[2] Hefei National Research Center for Physical Sciences at the Microscale, University of Science and Technology of China, Hefei 230026, People's Republic of China
[3] Hefei National Laboratory, University of Science and Technology of China, Hefei 230088, People's Republic of China
[*] Author to whom any correspondence should be addressed.

E-mail: jinwang@ustc.edu.cn

Keywords: electric polarizability, optical refractometer, gas metrology

Abstract

We report high-precision measurements of the static electric dipole polarizabilities for methane (CH_4), carbon monoxide (CO), and oxygen (O_2) using an optical refractometer operating at 1566 nm. The dynamic polarizabilities at 1566 nm were converted to static polarizabilities via dipole oscillator strength distributions. The resulting static polarizabilities are 6.440 34(30) for CH_4, 4.881 46(24) for CO, and 3.958 19(20) for O_2, corresponding to relative standard uncertainties of 45 ppm, 49 ppm, and 46 ppm, respectively. The value obtained for O_2 shows excellent agreement with the literature value of 3.9582(2), while those for CH_4 and CO represent an improvement in precision by more than two orders of magnitude. These data provide a reliable benchmark for molecular polarizability calculations and contribute to accurate modeling of intermolecular dispersion forces and gas metrology.

1. Introduction

The electric dipole polarizability is a fundamental physical quantity that characterizes the response of the electron cloud of a molecule or atom to an applied static electric field. It plays a crucial role in both theoretical calculations and practical applications, as it is directly related to optical properties such as the refractive index (RI) and dielectric constant, and serves as a key parameter for calculating intermolecular forces such as dispersion interactions [1, 2]. Dispersion forces, which are long-range interactions dominated by dynamic electron correlation, are essential in chemical, physical, and biological systems, profoundly influencing processes such as protein folding, surface adsorption, and material assembly [1–3]. The C_6 and C_9 dispersion coefficients are critical parameters for describing such intermolecular dispersion interactions, possessing clear physical significance and practical value. Accurate static polarizabilities are the starting point for calculating these dispersion coefficients [4, 5].

On the theoretical side, various methods such as time-dependent configuration interaction [6], the algebraic-diagrammatic construction scheme [1], and time-dependent density functional theory [2], have been developed to predict polarizabilities accurately. Even the quantum electrodynamics contribution has been included in the high-precision calculation [7, 8] of the dipole polarizability of atomic helium. Experimentally, several techniques are available for determining the static polarizabilities of gaseous molecules, including dielectric permittivity (DP) measurements [9–11], RI gas metrology [12–15], molecular beam deflection [16], and matter-wave interferometry [17]. However, for molecules, the most accurate measurements have primarily come from dielectric constant and RI methods.

In recent years, RI measurements have achieved ppm-level precision for polarizabilities of some noble gases and simple molecules [12, 14, 15, 18–20]. Nevertheless, for key atmospheric molecules such as CH_4, CO, and O_2, which are vital in energy, chemical engineering, and fundamental physics, the exist-

ing precision of static polarizability measurements remains limited. Apart from oxygen, which has high-precision dielectric experimental results [9], the relative uncertainties for the other two molecules are greater than 10^{-3}, and discrepancies persist between theoretical calculations and experimental results for methane [6]. This limitation hampers the use of polarizabilities as accurate descriptors for predicting intermolecular forces through C_6 and C_9 coefficients. For instance, in optimizing industrial separation models, Pribylov and Murdmaa [21] reported a 7% error in adsorption separation designs based on polarizability differences between CH_4 and other hydrocarbons, which could be improved with more precise polarizability data.

Therefore, high-precision determinations of the polarizabilities of CH_4, CO, and O_2 with greater confidence are essential. Such measurements not only provide cross-validation of previous results but also serve to test theoretical calculations. The precise determination of molecular polarizability enables a highly sensitive, non-invasive method for gas pressure and composition analysis. This approach supports unmanned atmospheric monitoring in harsh environments, allowing integrated vertical pressure profiling from ground level to high altitudes. In mixed gas analysis, it facilitates rapid, high-precision quantification of nitrogen, oxygen, carbon dioxide, methane, etc with calibration accuracy at the ppm level or even beyond. Applications span gas metrology, chemical process control, environmental monitoring, and semiconductor gas quality control.

2. Experimental

2.1. Optical refractometer

The experiment is based on a high-precision gas optical refractometer (figure 1), whose core is a Fabry–Pérot interferometer cavity made of ultra-low expansion (ULE) glass with a length of 10 cm. Both ends of the cavity are equipped with high-reflectivity mirrors (reflectivity $R \approx 99.9\%$). The relationship between the cavity mode frequency and the RI of the gas inside the cavity is given by [14, 18]:

$$n - 1 = \frac{\Delta\nu}{\nu_{\mathrm{f}}} + \Delta p \left(\frac{1}{3K} + d \right), \qquad (1)$$

where ν_{f} is the resonance frequency of the optical cavity filled with gas, $\Delta\nu$ is the change in the cavity mode frequency before and after gas filling, and Δp is the corresponding pressure change inside the cavity. K is the bulk modulus of the cavity material; for the ULE glass used in this setup, $K \approx 3.3 \times 10^{10}$ Pa. The parameter d is a correction factor accounting for mirror deformation under pressure [22], with units of Pa^{-1}.

The apparatus determines the RI of high-purity gas by precisely measuring the absolute change in the resonance frequency of the optical cavity before and after gas introduction. The light source is a fiber laser operating at 1566 nm (Precilaser, linewidth <10 kHz), which is stabilized to a longitudinal mode of the cavity using the Pound–Drever–Hall active locking technique. The free spectral range of the resonator is 1.5 GHz, and the cavity mode linewidth is approximately 0.4 MHz. The cavity is sealed inside a stainless steel vacuum chamber, which is housed within an aluminum alloy temperature-stabilized jacket. The operating temperature is maintained at approximately 297.53 K by a high-precision PID controller. The cavity temperature is monitored in real time using a platinum resistance thermometer calibrated by the National Institute of Metrology (NIM) of China, with a measurement uncertainty of 5 mK.

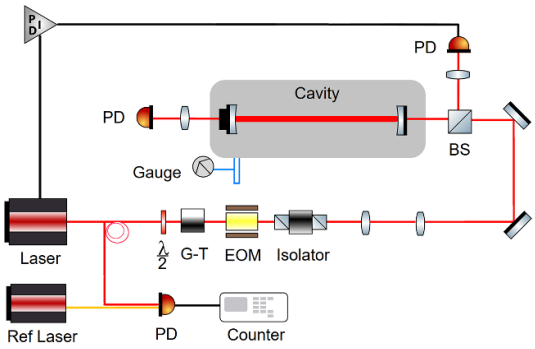

Figure 1. Schematic of the experimental setup.

The absolute cavity mode frequency is measured by optical heterodyne beating with an ultra-stable reference laser system, whose frequency is locked to an ultra-stable optical cavity maintained under high vacuum. Long-term comparison with an optical frequency comb shows a frequency drift rate lower than $0.1\,\mathrm{Hz\,s^{-1}}$. Gas pressure is measured using a commercial capacitance diaphragm gauge (Inficon Cube CDGSci, 1000 Torr full scale, with a manufacturer-specified accuracy of 0.025%). The pressure gauge was calibrated against a Fluke PG7601 piston gauge (traceable to the national pressure standard with a standard uncertainty of 11 ppm, $k = 1$), establishing a complete pressure traceability chain.

Both cavities are made of the same ULE material. Cavity 1 uses ULE-based mirrors, which are identical to the cavity material, so mirror deformation is negligible. Cavity 2 employs quartz-based mirrors, requiring consideration of mirror deformation. The bulk modulus K and the mirror deformation coefficient d for the ULE cavity were calibrated by measuring the RI of nitrogen ($A_\varepsilon = 4.387\,05(16)\ \mathrm{cm^3 \cdot mol^{-1}}$ [12]). After calibration, we obtained $K_1 = K_2 = 3.0822 \times 10^{10}$ Pa and $d = -2.0293 \times 10^{-13}$ Pa. The measurement error of the optical pressure gauge is within $u_{\mathrm{opt}} = \sqrt{(20 \times 10^{-6} p)^2 + (4\,\mathrm{mPa})^2}$, $k = 1$.

Table 1. Dipole sum terms [29–31] and virial coefficients for the gases studied. B_T values are from [32, 33]; B_ε values are from [34–36]; A_μ values are from [37–39].

	CH_4	O_2	CO
$S(-4)$ (a.u.)	62.22(19)	34.81(35)	48.26(48)
$S(-6)$ (a.u.)	295.0(57)	238.6(23)	292.9(29)
$S(-8)$ (a.u.)	1660(54)	2224(66)	2308(64)
$A_\mu \times 10^6$ ($cm^3 \cdot mol^{-1}$)	−17.4(8)	3449(34)	−15.65(24)
B_T ($cm^3 \cdot mol^{-1}$)	42.3(7)	−15.7(1)	−8.5(2)
B_ε ($cm^6 \cdot mol^{-2}$)	7.29(32)	−0.305(28)	7.97(40)

By tracing the measurements of optical frequency, gas pressure, and thermodynamic temperature directly to SI units, the apparatus enables precise determination of gas polarizabilities. Two independent optical refractometers were constructed [23, 24], and their long-term stability was verified through mutual comparison. Prior to this experiment, observations over more than a year in the pressure range of 2 kPa to 100 kPa showed that measurement deviations remained within a 20 ppm uncertainty range [12]. After calibration with the optical pressure gauge, the combined relative standard uncertainty of the pressure measurement system (using the commercial Inficon diaphragm gauge) within 100 kPa is given by $u_{cap} = \sqrt{(20 \times 10^{-6} p)^2 + (1.5\,\mathrm{Pa})^2}$.

2.2. Polarizability measurement

This experiment measures the polarizabilities of several gas molecules using the optical pressure gauge described above, based on the optical refractometry method. The principle relies on precise measurements of the gas RI n, pressure, and temperature, through the formula [25, 26]:

$$\frac{p}{RT} = \frac{2(n-1)}{3(A_\varepsilon + A_\mu)} + (n-1)^2 \times \left[\frac{4B_T}{9(A_\varepsilon + A_\mu)^2} - \frac{A_\varepsilon^2 + 4B_\varepsilon + 6A_\varepsilon + A_\mu}{9(A_\varepsilon + A_\mu)^3}\right] + O(n-1)^3. \quad (2)$$

In this equation, p is the gas pressure (in Pa), measured in real time by the capacitance diaphragm gauge calibrated with the optical pressure gauge; R is the molar gas constant, $R = 8.314\,4626$ $J \cdot mol^{-1} \cdot K^{-1}$; T is the thermodynamic temperature (in K) measured by the calibrated platinum resistance thermometer; n is the RI of the gas; A_ε is the molar electric dipole polarizability (static electric dipole polarizability) in $cm^3 \cdot mol^{-1}$; A_μ is the molar magnetic polarizability in $cm^3 \cdot mol^{-1}$; B_T is the second virial coefficient in $cm^3 \cdot mol^{-1}$; and B_ε is the second dielectric virial coefficient in $cm^6 \cdot mol^{-2}$.

We measure the molar polarizability at a wavelength of 1566 nm, which is related to the static polarizability and the frequency-dependent dynamic polarizability through the following relation:

$$A'_\varepsilon(\omega) = A_\varepsilon + \frac{4}{3}\pi N_A a_0^3 \left(1 + \frac{m_e}{m_w}\right)^3 \times \left[S(-4)\omega^2 + S(-6)\omega^4 + S(-8)\omega^6\right]. \quad (3)$$

Here, $A'_\varepsilon(\omega)$ is the dynamic polarizability as a function of angular frequency, which is the quantity determined experimentally; A_ε is the static polarizability; N_A is Avogadro's constant; a_0 is the Bohr radius; m_e is the electron mass; m_w is the nuclear mass; ω is the angular frequency of the laser in atomic units, with $\omega = 45.563\,978\,23/\lambda$, where λ is the vacuum wavelength. $S(-4)$, $S(-6)$, and $S(-8)$ are dipole sums in atomic units (a.u.), which can be calculated from the dipole oscillator strength distribution (DOSD) [27, 28]. The values for methane, carbon monoxide, and oxygen are listed in table 1. Additionally, the corresponding virial coefficients and other parameters for these gases are provided in the same table.

2.3. Uncertainty assessment

The overall uncertainty budget is summarized in table 2. The cavity temperature was measured using a platinum resistance thermometer calibrated by the NIM of China, with an uncertainty lower than 5 mK, contributing a relative standard uncertainty of 16 ppm to the polarizability measurement. The pressure measurement uncertainty, as presented in the previous section, is 25 ppm at 1 bar. In this measurement, CH_4 and CO samples with a purity of 99.999%, and O_2 samples with a purity of 99.9995% were used, resulting in relative standard uncertainties due to gas purity of less than 10 ppm.

Outgassing from the cavity vacuum also affects the measurement. We tested this by measuring the frequency drift with the valve between the vacuum line and the cavity closed; the drift rate was approximately 4 $Hz\,s^{-1}$. We also observed fluctuations of about 2 kHz in the recorded phase-locked frequency, which may originate from temperature-dependent drifts in the PDH locking servo reference. At 1 bar, the frequency shifts $\Delta\nu$ for CH_4, CO, and O_2 are approximately 75 GHz, 54 GHz, and 44 GHz, respectively. Over several hours of measurement, the relative uncertainty due to cavity outgassing at each pressure point

Table 2. Uncertainty budget for the static polarizabilities of CH_4, CO, and O_2. All fractional uncertainties in 10^{-6} (ppm, $k = 1$).

	CH_4	O_2	CO
T	16	16	16
P	25	25	25
$S(i)$	9	28	31
B	28	11	20
A_μ	0.6	8	0.2
Statistical	14	17	7
Gas purity	10	5	10
Out gassing	0.1	0.2	0.2
Cavity thermal expansion	<0.1	<0.1	<0.1
Optical frequency fluctuation	<0.1	<0.1	<0.1
Total	45	46	49

was below 0.2 ppm. The thermal expansion coefficient of the ULE cavity at the experimental temperature is $3 \times 10^{-9}\,K^{-1}$. Considering the temperature uncertainty of 5 mK, the effect of cavity thermal expansion on the polarizability determination was assessed to be below 0.1 ppm.

The second dielectric virial coefficient B_ε and the second virial coefficient B_T are temperature-dependent, and their contributions to the overall uncertainty increase with pressure. Their values and references have been provided earlier. Their relative standard uncertainties for CH_4, CO, and O_2 are 28 ppm, 20 ppm, and 11 ppm, respectively. The uncertainties of the dipole sum terms $S(i)$ $(i = -4, -6, -8)$ given in table 1 also contribute to the total uncertainty when converting the dynamic polarizability measured at 1566 nm to the static polarizability. According to equation (3), their relative standard uncertainties for CH_4, CO, and O_2 are 9 ppm, 31 ppm, and 28 ppm, respectively.

For the molecules of interest, the magnetic polarizability A_μ of CH_4 and CO is only 10^{-6} times their electric polarizability A_ε, contributing an error of less than 1 ppm to the polarizability. O_2, as a strong paramagnetic molecule, has a magnetic polarizability A_μ that is 10^{-4} times its electric polarizability A_ε, contributing an error of 8 ppm.

It is noted that both CO and CH_4 have resonant absorption in the near-infrared region. Near absorption peaks, the polarizability of the gas can be affected. To evaluate this effect, we used CO as an example (due to its stronger absorption) and performed additional measurements with the laser frequency offset by 30 GHz from the nominal wavelength. The difference between the two results was $9 \times 10^{-5}\,cm^3{\cdot}mol^{-1}$, indicating that the influence of resonant absorption lines on the polarizability data is less than 20 ppm.

3. Results and discussion

3.1. CH_4

We measured the molar polarizability of CH_4 at various pressure points in the range of 2 kPa to 100 kPa at a wavelength of 1566 nm. The static polarizability was derived at each pressure point using the formulas described above. Due to the larger relative uncertainty in pressure measurement at low pressures, the uncertainties of these data points are also greater. The weighted average and its 1σ confidence interval across different pressure points are indicated by the dashed line and purple band, respectively. The relative uncertainty of the weighted average is 45 ppm.

In fact, the available reference results for CH_4 are limited in precision, and both experimental and theoretical results mostly date back to the last century. Referring to the CH_4 polarizability data summarized in the review by Olney *et al* [29], the values obtained by the RI method range from 6.39 to 6.46 $cm^3{\cdot}mol^{-1}$. Our result falls within this range, although conditions such as temperature that affect molecular populations are difficult to evaluate. Modern computational methods, such as those used by Ulusoy *et al* [6] with different basis sets, yield results in the range of 6.246 to 6.337 $cm^3{\cdot}mol^{-1}$. The authors noted that achieving better accuracy is computationally challenging, making modern theoretical results difficult to use as a reference for our experiment.

For the reasons stated above, we compare our results with the summary by Hohm, which provides static polarizabilities obtained from both RI and DP measurements. The uncertainties are relatively good and mostly represent averages from various literature sources. It is worth noting that the DP method typically operates in the GHz frequency range, so we consider the dynamic contribution from ω to be approximately zero. Figure 2(d) compares our results with literature values. The RI and DP results [40] are $6.445(10)\,cm^3{\cdot}mol^{-1}$ and $6.454(17)\,cm^3{\cdot}mol^{-1}$, respectively. Compared with our value of $6.440\,34(30)\,cm^3{\cdot}mol^{-1}$, the relative deviations are 0.08% and 0.2%, which agree within the respective uncertainties. As noted by Hohm, the measured polarizability depends on temperature due to vibrational and rotational excitations of

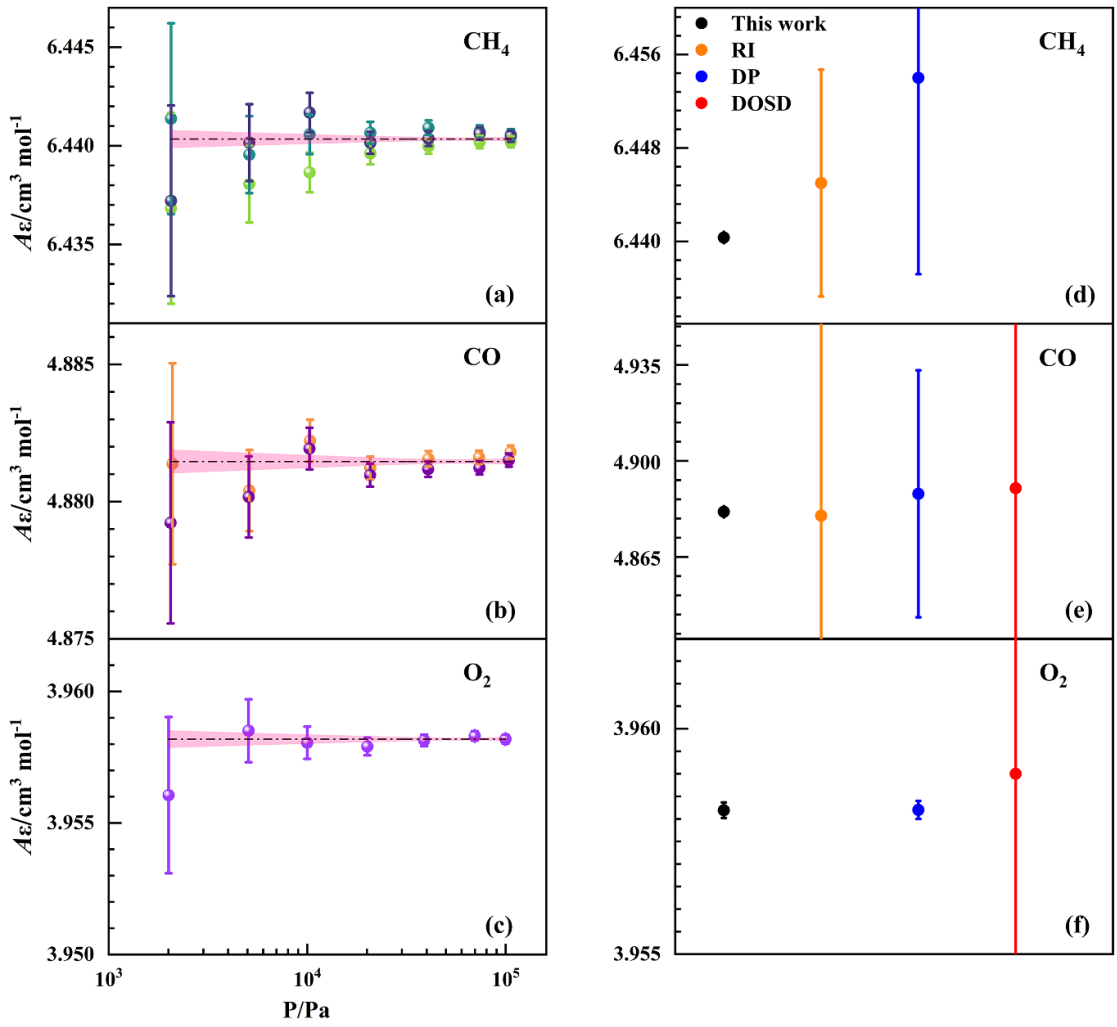

Figure 2. (a) CH_4, (b) CO, and (c) O_2: static polarizabilities as a function of pressure, derived from dynamic measurements at a wavelength of 1566 nm. Different colors represent multiple repeated measurements, and the shaded regions indicate the 1σ confidence interval of the mean. (d) CH_4, (e) CO, and (f) O_2: comparison of static polarizabilities with literature values. Different colors represent different data sources: refractive index (RI) experiments (orange), dielectric permittivity (DP) experiments (blue), and dipole oscillator strength distribution (DOSD) calculations (red).

the molecules [41, 42]. Fortunately, this effect is small, approximately 5–10 ppm per K [40, 43], and remains consistent with the reference data within uncertainties for deviations of a few K at room temperature.

3.2. CO

We measured the molar polarizability of CO at the same pressure points in the range of 2 kPa to 100 kPa. The static polarizability was derived at each pressure point using the formulas described above. The weighted average and its uncertainty at 1566 nm are shown by the dashed line and purple band, with an uncertainty of 46 ppm.

Figure 2(f) compares our results with literature values. When a molecule is placed in an electric field, its polarizability comprises three contributions: vibrational, electronic, and orientational. RI measurements are performed at high frequencies where vibrations cannot respond to the electric field; therefore, the RI method essentially measures the electronic part of the molecular polarizability. To better compare with other literature results, we refer to the correction for vibrational contributions by Bishop and Cheung [44], who estimated the vibrational contribution as $20(1) \times 10^{-43}\ C^2{\cdot}m^2{\cdot}J^{-1}$. By subtracting this difference, we convert literature results to the electronic part for comparison with our data. The DP results for CO also include an orientational contribution due to its permanent dipole moment. Using the experimental result $\mu_e = 0.107(1)$ D from Tsankova *et al* [10], we subtracted the orientational contribution. Additionally, we interpolated the experimental data at 255, 273, 293, and 313 K to estimate the value at 297 K.

The RI [40] and DP [10] results are $4.88(26)\ cm^3{\cdot}mol^{-1}$ and $4.888(45)\ cm^3{\cdot}mol^{-1}$, respectively. The DOSD computational result

Table 3. Experimental derived static polarizabilities (A_ε) for CH_4, CO, and O_2, compared with values obtained from RI [40], DP [9, 10, 40], and DOSD [30, 31] methods (units: $cm^3 \cdot mol^{-1}$).

	CH_4	CO	O_2
This work	6.440 34(30)	4.881 46(24)	3.958 19(20)
RI	6.445(10)	4.88(26)	—
DP	6.454(17)	4.888(45)	3.9582(2)
DOSD	—	4.89(53)	3.959(11)

is 4.89(53) $cm^3 \cdot mol^{-1}$. All of these agree with our experimental result within the respective uncertainties.

3.3. O_2

We measured the molar polarizability of O_2 at the same pressure points in the range of 2 kPa to 100 kPa. The static polarizability was derived at each pressure point using the formulas described above. The weighted average and its uncertainty at 1566 nm are shown by the dashed line and purple band, with an uncertainty of 49 ppm.

Figure 2(e) compares our results with literature values. May *et al* obtained high-precision static polarizabilities for O_2 at 273, 293, and 323 K using the DP method [9]. We estimated the value at 297 K by interpolation, since the results at 293 and 323 K are 3.9582(2) $cm^3 \cdot mol^{-1}$ and 3.95824(7) $cm^3 \cdot mol^{-1}$, respectively. Taking the uncertainty from the 293 K result as reference, the interpolated value is 3.9582(2) $cm^3 \cdot mol^{-1}$, which agrees at the 10^{-5} level with our result of 3.95819(20) $cm^3 \cdot mol^{-1}$. It is also consistent with the DOSD computational result of 3.959(11) $cm^3 \cdot mol^{-1}$ [31].

4. Conclusion

This study employed high-precision optical refractometry to measure the dynamic polarizabilities of CH_4, CO, and O_2 at a wavelength of 1566 nm, which were then converted to static polarizabilities using DOSD theory. The refractometer achieved measurement uncertainties at the level of several tens of ppm. The final results are compared with literature values in table 3. The results show that the static polarizabilities obtained in this work are consistent with literature values from both the RI and DP methods within their respective uncertainties, while improving the precision by approximately an order of magnitude. This work provides highly accurate experimental data for the polarizabilities of these gases, offering a valuable reference for future studies.

Acknowledgments

This work was supported by the Independent Deployment Project of HFNL (Grant No. ZB2025010500), National Natural Science Foundation of China (Grant No. 12393825), Chinese Academy of Sciences (Grant Nos. XDA0520304, XDB0970100), and the Quantum Science and Technology-National Science and Technology Major Project (Grant No. 2021ZD0303102).

References

[1] Fransson T, Rehn D R, Dreuw A and Norman P 2017 Static polarizabilities and C_6 dispersion coefficients using the algebraic-diagrammatic construction scheme for the complex polarization propagator *J. Chem. Phys.* **146** 20519
[2] Abella L and Autschbach J 2022 Density functional response calculations of dispersion coefficients C_6 and C_9 of closed- and open-shell systems *J. Phys. Chem.* A **126** 5821
[3] Klimeš J and Michaelides A 2012 Perspective: Advances and challenges in treating van der Waals dispersion forces in density functional theory *J. Chem. Phys.* **137** 120901
[4] Leech J W 1948 The influence of retardation on the London–van der Waals forces *Phil. Mag.* **46** 1328
[5] Gould T and Bučko T 2016 C_6 coefficients and dipole polarizabilities for all atoms and many ions in rows 1-6 of the periodic table *J. Comput. Theory Chem.* **12** 3603
[6] Ulusoy I S, Stewart Z and Wilson A K 2018 The role of the CI expansion length in time-dependent studies *J. Chem. Phys.* **148** 14107
[7] Puchalski M, Szalewicz K, Lesiuk M and Jeziorski B 2020 QED calculation of the dipole polarizability of helium atom *Phys. Rev.* A **101** 022505
[8] Lesiuk M and Jeziorski B 2023 First-principles calculation of the frequency-dependent dipole polarizability of argon *Phys. Rev.* A **107** 042805
[9] May E F, Moldover M R and Schmidt J W 2008 Electric and magnetic susceptibilities of gaseous oxygen: present data and modern theory compared *Phys. Rev. A* **78** 4061
[10] Tsankova G, Richter M, Stanwix P L, May E F and Span R 2018 Accurate high-pressure measurements of carbon monoxide's electrical properties *Chem. Phys. Chem.* **19** 784
[11] Gaiser C and Fellmuth B 2018 Polarizability of helium, neon and argon: new perspectives for gas metrology *Phys. Rev. Lett.* **120** 123203
[12] Nie Z-L, Wang J, Hu C-L, Sun Y R, Cheng C-F, Tan Y and Hu S-M 2025 Polarizability of molecular hydrogen and gas metrology *Phys. Rev.* A **111** 012801
[13] Stone J A and Stejskal A 2004 Using helium as a standard of refractive index: Correcting errors in a gas refractometer *Metrologia* **41** 189
[14] Egan P and Stone J A 2011 Absolute refractometry of dry gas to ±3 parts in 10^9 *Appl. Opt.* **50** 3076
[15] Yang Y, Stone J A and Egan P F 2025 Demonstration of dispersion gas barometry *Phys. Rev. Appl.* **23** 064041
[16] Götz D A, Heiles S and Schäfer R 2012 Polarizabilities of Si_N ($N = 8$–75) clusters from molecular beam electric deflection experiments *Eur. Phys. J.* D **66** 293
[17] Berninger M, Stefanov A, Deachapunya S and Arndt M 2007 Polarizability measurements of a molecule via a near-field matter-wave interferometer *Phys. Rev.* A **76** 013607
[18] Pendrill L R 2004 Refractometry and gas density *Metrologia* **41** S40
[19] Silander I, Zakrisson J, Axner O and Zelan M 2024 Realization of the pascal based on argon using a Fabry-Perot refractometer *Opt. Lett.* **49** 3296

[20] Zakrisson J, Silander I, Zelan M and Axner O 2025 Gouy phase in the presence of gas in Fabry-Perot refractometers *Opt. Expr.* **33** 12914
[21] Pribylov A A and Murdmaa K O 2023 Adsorption of n-alkanes on carbon adsorbents at high temperatures *Russ. Chem. Bull.* **72** 1107
[22] Takei Y, Telada S, Yoshida H, Arai K and Kobata T 2020 In-situ measurement of mirror deformation using dual Fabry–Pérot cavities for optical pressure standard *Measurement* **173** 108496
[23] Xu Y-R, Liu Y-Y, Wang J, Sun Y, Xi Z-H, Li D-T and Hu S-M 2020 Vacuum metrology based on refractive index of gas *Acta Phys. Sin.* **69** 150601
[24] Liu Y-Y, Hu C-L, Sun Y, Wang J and Hu S-M 2022 Measurement of gas pressure by double-cavity comparison refractive index method *Acta Phys. Sin.* **71** 080601
[25] Rourke P M C, Gaiser C, Gao B, Ripa D M, Moldover M R, Pitre L and Underwood R J 2019 Refractive-index gas thermometry *Metrologia* **56** 032001
[26] Rourke P M C 2021 Perspective on the refractive-index gas metrology data landscape *J. Phys. Chem. Ref. Data* **50** 033104
[27] Thakkar A J, Hettema H and Wormer P E S 1992 Ab initio dispersion coefficients for interactions involving rare-gas atoms *J. Chem. Phys.* **97** 3252
[28] Bulanin M and Kislyakov I 1999 Dynamic polarizabilities of rare-gas atoms: helium, neon and argon *Opt. Spectrosc.* **86** 632
[29] Olney T N, Cann N, Cooper G and Brion C 1997 Absolute scale determination for photoabsorption spectra and the calculation of molecular properties using dipole sum-rules *Chem. Phys.* **223** 59
[30] Kumar A and Meath W J 1994 Reliable isotropic and anisotropic dipole properties and dipolar dispersion energy coefficients, for CO evaluated using constrained dipole oscillator strength techniques *Chem. Phys.* **189** 467
[31] Kumar A and Thakkar A J 2011 Ozone: Unresolved discrepancies for dipole oscillator strength distributions, dipole sums and van der Waals coefficients *J. Chem. Phys.* **135** 325
[32] Barreiros S F, Calado J C G, Ponte M N D and Saville G 1987 Second virial coefficients of carbon monoxide *J. Chem. Thermodyn.* **19** 941
[33] Sengers J L, Klein M and Gallagher J S 1971 Pressure-volume-temperature relationships of gases Virial coefficients (available at: https://api.semanticscholar.org/CorpusID:91603360)
[34] Bose T K, Sochanski J S and Cole R H 1972 Dielectric and pressure Virial coefficients of imperfect gases. V. Octopole moments of CH_4 and CF_4 *J. Chem. Phys.* **57** 3592
[35] Stone A J, Tantirungrotechai Y and Buckingham A D 2000 The dielectric virial coefficient and model intermolecular potentials *Phys. Chem. Chem. Phys.* **2** 429
[36] Schmidt J W and Moldover M R 2003 Dielectric permittivity of eight gases measured with cross capacitors *Int. J. Thermophys.* **24** 375
[37] Barter C, Meisenheimer R G and Stevenson D P 1960 Diamagnetic susceptibilities of simple hydrocarbons and volatile hydrides *J. Chem. Phys.* **64** 1312
[38] Karplus M and Kolker H J 1963 Magnetic susceptibility of diatomic molecules *J. Chem. Phys.* **38** 1263
[39] Haynes W M (ed) 2011 *CRC Handbook of Chemistry and Physics* 92nd edn (CRC Press) p 2656
[40] Hohm U 2013 Experimental static dipole–dipole polarizabilities of molecules *J. Mol. Struct.* **1054–1055** 282
[41] Petrakis L and Sederholm C H 1961 Temperature-dependent chemical shifts in the NMR spectra of gases *J. Chem. Phys.* **35** 1174
[42] Bell P R 1942 Polarisibility and internuclear distance *Trans. Faraday Soc.* **38** 422
[43] Hohm U and Trümper U 1995 Frequency dependence of the polarizability derivative $[\partial\alpha(\omega)/\partial r]_0$ of chlorine from temperature-dependent gas-phase refractive index measurements *J. Raman Spectrosc.* **26** 1059
[44] Bishop D M and Cheung L M 1982 Vibrational contributions to molecular dipole polarizabilities *J. Phys. Chem. Ref. Data* **11** 119